ELSEVIER

Biophysical Chemistry 115 (2005) 67–76

Biophysical Chemistry

http://www.elsevier.com/locate/biophyschem

Stopped-flow studies of guanine binding by calf spleen purine nucleoside phosphorylase

M. Długosz, A. Bzowska, J.M. Antosiewicz*

Department of Biophysics, Warsaw University, Zwirki i Wigury 93 St., Warsaw 02-089, Poland

Received 11 October 2004; received in revised form 7 January 2005; accepted 14 January 2005
Available online 28 January 2005

Abstract

The binding of guanine to calf spleen purine nucleoside phosphorylase at 20 °C, in 20 mM Hepes–NaOH buffer, pH 7.0, at several ionic strength between 5 and 150 mM was investigated using a stopped-flow spectrofluorimeter. The kinetic transients registered after mixing a protein solution with ligand solutions of different concentrations were simultaneously fitted by several association reaction models using nonlinear least-squares procedure based on numerical integration of the chemical kinetic equations appropriate for given model. It is concluded that binding of a guanine molecule by each of the binding sites is a two-step process and that symmetrical trimeric calf spleen purine nucleoside phosphorylase represents a system of (identical) interacting binding sites. The interaction is visible through relations between the rate constants and non-additivity of changes in "molar" fluorescence for different forms of PNP–guanine complexes. It is also probable that electrostatic effects in guanine binding are weak, which indicates that it is the neutral form of the ligand which is bound and dissociated by PNP molecule.

Keywords: PNP; Guanine; Fluorescence; Stopped-flow; Numerical integration

1. Introduction

Purine nucleoside phosphorylase (PNP, E.C. 2.4.2.1) is a ubiquitous enzyme of the purine salvage metabolic pathway. In eukaryotes and in some bacteria trimeric enzyme is present which catalyses the reversible phosphorolysis of 6-oxo-purine ribo- and 2′-deoxyribonucleosides, as follows: β-(deoxy)-nucleoside+phosphate↔purine+α-(deoxy)-ribose-1-phosphate. Potent inhibitors of human and parasitic PNPs are considered potential immunosuppressive and anti-parasitic agents [1].

Even though the biological importance of PNP is recognized, the kinetic mechanism of the enzyme is not yet fully characterized [2,3]. In this study we analyse certain aspects of this mechanism, namely binding of guanine by calf spleen PNP in the absence of phosphate, using stopped-flow spectrofluorimetry methods. A ribbon model of calf spleen PNP molecule, crystallized with hypoxanthine as the ligand, is presented in Fig. 1 [4]. Each trimeric PNP molecule (P) contains three sites for the ligand (L). Guanine molecules are probably bound by the same three binding sites. Because of the symmetry of the PNP trimer, the protein can be considered as a macromolecule with three identical either noninteracting or interacting sites.

Binding of various ligands by trimeric PNPs (calf and Cellulomonas) is accompanied by 1–15% change in the intensity of the enzyme intrinsic fluorescence as a result of changes in tryptophan/tyrosine conformations and/or molecular environment. By contrast, interaction with guanine (in the absence of phosphate) results in puzzling enhancement of enzyme emission as high as 70% (calf spleen PNP) and 76% (Cellulomonas PNP) with maximum at about 332–334 nm (excitation at 280 nm), hence near that of the intrinsic enzyme fluorescence [2,5]. This points to some possible contribution of the bound guanine to the observed fluorescence. First, it was attributed [2] to be due to preferential binding of anionic form of guanine (pKa~9.2, involving dissociation of the

* Corresponding author.
E-mail address: jantosi@biogeo.uw.edu.pl (J.M. Antosiewicz).

0301-4622/$ - see front matter © 2005 Elsevier B.V. All rights reserved.
doi:10.1016/j.bpc.2005.01.005

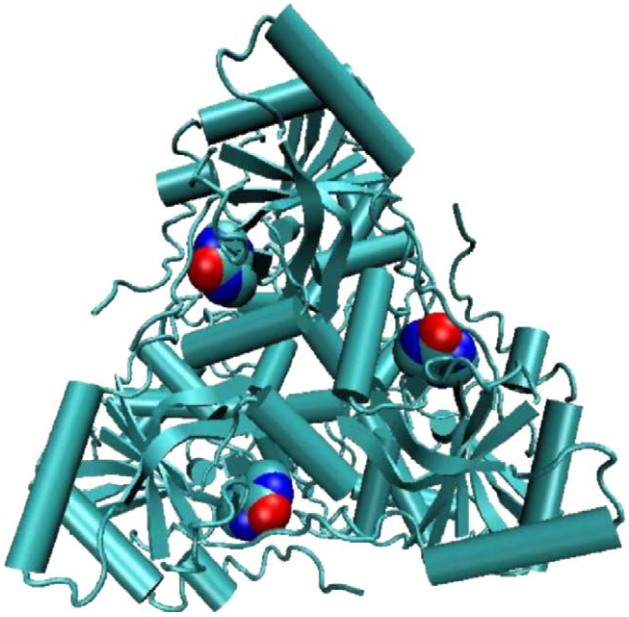

Fig. 1. Ribbon image of the trimeric calf spleen PNP molecule (cartoon representation) complexed with hypoxanthine (CPK representation). The figure was prepared using program VMD [12] and coordinates of the protein available from Protein Data Bank under accession code 1VFN [4].

N(1)–H of purine), known to be highly fluorescent [6,7]. However, subsequent spectroscopic and X-ray diffraction studies, including those that propose molecular mechanism of catalysis in which crucial role of N(1)–H. . .Glu201 (Glu204 in the structurally similar trimeric Cellulomonas PNP) is postulated, do not support this hypothesis and rather point to preferential binding of some rare tautomeric or ionic fluorescent form of guanine [5,8,9].

The purpose of this study is to derive kinetic and optical parameters for a binding model appropriate for the symmetrical trimeric structure of the macromolecule, and based on these parameters, to conclude if the binding sites can be classified as interacting or noninteracting, and whether the electrostatic interactions play any significant role in the complex formation by PNP and guanine.

2. Materials and methods

2.1. Materials

Calf spleen PNP (20–34 U/mg) and xanthine oxidase from buttermilk (~1 U/mg), suspensions in 3.2 M and 2.3 M ammonium sulphate, respectively, inosine (Ino), Hepes (ultra pure), Na_2HPO_4, NaH_2PO_4 and guanine (Gua) were products of Sigma. The commercial calf spleen PNP was desalted by extensive washing (8 times) on Centricon centrifugal filter devices YM-30 (2 ml) with 30 kDa cuf-off (Millipore) as described previously [3]. Specific activity of the enzyme was determined by the standard coupled xanthine oxidase procedure with λ_{obs}=300 nm and $\Delta\epsilon$=9 600 M^{-1} cm^{-1} [10]. Guanine is poorly soluble in water at neutral pH. Therefore, to obtain high guanine concentrations necessary for stopped-flow experiments ~1.8 mM solution of guanine in 3 mM NaOH was prepared and subsequently mixed with Hepes pH 7.0 to get a desired concentration. It was confirmed that the amount of NaOH added does not affect the final pH.

2.2. Instrumentation

Spectrophotometric measurements were carried out on a Uvikon 930 (Kontron, Austria) spectrophotometer fitted with a thermostatically controlled cell compartment, using 10-, 2- or 1-mm path-length quartz cuvettes (Hellma, Germany). A Beckman model Φ300 pH-meter equipped with a combined semi-microelectrode and temperature sensor was used for pH determination. Stopped-flow kinetic measurements were run on a SX.18MV stopped-flow reaction analyser from Applied Photophysics Ltd.

2.3. Stopped-flow measurements

Emission of PNP and PNP–guanine complexes was excited at 290 nm (slit widths=0.5 mm=2.32 nm), and their fluorescence was monitored with cut-off filter 320 nm. Extinction and emission path lengths in the stopped-flow cell were 2 mm and 10 mm, respectively. The investigated reactions consisted of mixing equal volumes of ~2.31 μM/monomer PNP (0.77 μM trimer, determined by absorption measurements, using $\epsilon_{1\%,280nm}$=9.6 [3]) solution with guanine solution with a concentration between 1 and 30 μM, at 20 °C, in 20 mM Hepes buffer, pH 7.0, and KCl added, to obtain a desired ionic strength of the solution (4.8, 25, 50, 100 and 150 mM). Contribution of the 20 mM Hepes at pH 7 to the ionic strength was estimated as 4.8 mM. Six concentrations of the ligand were used: 1.25, 2.5, 5.0, 10.0, 20.0, and 30.0 μM. One thousand data points were recorded over the course of each reaction using oversampling option of the instrument, and twelve runs were averaged for each concentration of the reagents. The concentrations listed above refer to situation prior mixing in the stopped-flow apparatus (in the apparatus syringes). All solutions were filtered prior concentration determination and subsequently degassed before placing them into the stopped-flow syringes. The stopped-flow experiments were done in duplicate for two independent preparations of the solutions, just to check reproducibility of the experiments.

2.4. Analysis of stopped-flow data

Kinetic traces, resulting from the fluorescence increase accompanying binding of guanine to PNP, were analysed using a home written software, similar to that described previously [11]. Different types of models of the reaction scheme, each treating PNP molecule as a trimer with three identical binding sites, were assumed. Each model was related to experimental data assuming that at any given

moment of time the fluorescence of the solution can be represented as a sum of contributions due to distinguishable molecular species in the mixture, i.e. free protein and ligand molecules, and possible forms of their complexes:

$$F(t) = \sum_{\mathrm{x}} F_{\mathrm{x}} \cdot c_{\mathrm{x}}(t) \tag{1}$$

where c_{x} is the molar concentration of molecular species X and F_{x} is its "molar fluorescence" for given solution conditions and the spectrofluorimeter settings. Eq. (1), together with the integration of the kinetic differential equations appropriate for the mechanism of association, described below, allows one to determine the values of the optical and kinetic parameters characterizing the molecular species and their mutual conversions.

The simplest reaction scheme describing ligand binding by PNP, consistent with the structure of the protein, can be represented by the following three association steps:

$$\begin{aligned} &\mathrm{P} + \mathrm{L} \underset{k_{\mathrm{d1}}}{\overset{k_{\mathrm{a3}}}{\rightleftharpoons}} \mathrm{C1} \\ &\mathrm{C1} + \mathrm{L} \underset{k_{\mathrm{d2}}}{\overset{k_{\mathrm{a2}}}{\rightleftharpoons}} \mathrm{C2} \\ &\mathrm{C2} + \mathrm{L} \underset{k_{\mathrm{d3}}}{\overset{k_{\mathrm{a1}}}{\rightleftharpoons}} \mathrm{C3} \end{aligned} \tag{2}$$

where P is the free trimeric protein, L is the free ligand, CI is the complex of the protein with I ligand molecules occupying its binding sites, $k_{\mathrm{a}i}$ is the association rate constant when there are i empty sites on the protein, and $k_{\mathrm{d}i}$ is the dissociation rate constant when there are i occupied sites on the protein. One simple and obvious extension of the above model is to assume that association of a ligand molecule with a given binding site on PNP is followed by a conformational transformation. As possible binding of the next ligand molecule might either follow or precede this transformation, the appropriate reaction scheme can be described by a two-dimensional reaction equation, which reads:

$$\begin{array}{ccccc} \mathrm{P} + 3\mathrm{L} & \underset{k_{\mathrm{d1}}}{\overset{k_{\mathrm{a3}}}{\rightleftharpoons}} & \mathrm{C1} + 2\mathrm{L} & \underset{k_{\mathrm{d2}}}{\overset{k_{\mathrm{a2}}}{\rightleftharpoons}} & \mathrm{C2} + \mathrm{L} \\ & & k_{\mathrm{b1}} \Uparrow \Downarrow k_{\mathrm{f1}} & & k_{\mathrm{b1}} \Uparrow \Downarrow k_{\mathrm{f2}} \\ & & \mathrm{K1} + 2\mathrm{L} & \underset{k_{\mathrm{d1}}}{\overset{k_{\mathrm{a2}}}{\rightleftharpoons}} & \mathrm{C1K1} + \mathrm{L} \\ & & & & k_{\mathrm{b2}} \Uparrow \Downarrow k_{\mathrm{f1}} \\ & & & & \mathrm{K2} + \mathrm{L} \end{array} \quad \begin{array}{c} \underset{k_{\mathrm{d3}}}{\overset{k_{\mathrm{a1}}}{\rightleftharpoons}} \\ k_{\mathrm{b1}} \Uparrow \Downarrow k_{\mathrm{f3}} \\ \underset{k_{\mathrm{d2}}}{\overset{k_{\mathrm{a1}}}{\rightleftharpoons}} \\ k_{\mathrm{b2}} \Uparrow \Downarrow k_{\mathrm{f2}} \\ \underset{k_{\mathrm{d1}}}{\overset{k_{\mathrm{a1}}}{\rightleftharpoons}} \\ k_{\mathrm{b3}} \Uparrow \Downarrow k_{\mathrm{f1}} \end{array} \begin{array}{c} \mathrm{C3} \\ \\ \mathrm{C2K1} \\ \\ \mathrm{C1K2} \\ \\ \mathrm{K3} \end{array} \tag{3}$$

where symbols P and L have the same meaning as for Eq. (2), CI is the complex of the protein with I ligand molecules with all binding sites not undergoing conformational isomerization, KI is the complex of the protein with I ligand molecules with all binding sites after conformational isomerization, CIKJ is the complex of the protein with I+J ligand molecules, where I sites did not undergo the isomerization and J sites are after isomerization, $k_{\mathrm{a}i}$ has the same meaning as for Eq. (2), $k_{\mathrm{d}i}$ is the dissociation rate constant, $k_{\mathrm{f}i}$ is the transformation rate constant, and $k_{\mathrm{b}i}$ is the reverse transformation rate constant, all when there are i occupied and not transformed sites on the protein. It should be noticed that although the model described by Eq. (3) does allow for positive or negative cooperativity between the binding sites, i.e. their interaction, it assumes that the internal conformational transition does not influence ability of binding subsequent ligand. For example, it assumes the same association rate constant k_{a2} for going from C1 to C2, and for going from K1 to C1K1, and in general these two association reactions does not need to be characterized by the same rate constant. However, taking such effects into account would increase the total number of freely adjusted rate constants from 12 to 24. Another simple extension of the model described by Eq. (2) assumes that it is necessary for each binding site to undergo a conformational transition before a ligand molecule can be attached. Such types of protein-ligand associations are less common and we postpone investigation of this possibility to a future study.

The above two reaction models were used in interpretation of the kinetic traces registered for association of PNP with guanine in this work. The instantaneous concentrations of molecular species at any given moment of time, for the above models, were determined by simultaneous numerical solution of the set of differential equations appropriate for the assumed model of reactions. For the set of reactions expressed by Eq. (2) these differential equations read:

$$\frac{\mathrm{d}[\mathrm{P}]}{\mathrm{d}t} = -k_{\mathrm{a3}}[\mathrm{P}][\mathrm{L}] + k_{\mathrm{d1}}[\mathrm{C1}]$$

$$\begin{aligned} \frac{\mathrm{d}[\mathrm{L}]}{\mathrm{d}t} = &-k_{\mathrm{a3}}[\mathrm{P}][\mathrm{L}] + k_{\mathrm{d1}}[\mathrm{C1}] - k_{\mathrm{a2}}[\mathrm{C1}][\mathrm{L}] + k_{\mathrm{d2}}[\mathrm{C2}] \\ &- k_{\mathrm{a1}}[\mathrm{C2}][\mathrm{L}] + k_{\mathrm{d3}}[\mathrm{C3}] \end{aligned}$$

$$\frac{\mathrm{d}[\mathrm{C1}]}{\mathrm{d}t} = k_{\mathrm{a3}}[\mathrm{P}][\mathrm{L}] - k_{\mathrm{d1}}[\mathrm{C1}] - k_{\mathrm{a2}}[\mathrm{C1}][\mathrm{L}] + k_{\mathrm{d2}}[\mathrm{C2}]$$

$$\frac{\mathrm{d}[\mathrm{C2}]}{\mathrm{d}t} = k_{\mathrm{a2}}[\mathrm{C1}][\mathrm{L}] - k_{\mathrm{d2}}[\mathrm{C2}] - k_{\mathrm{a1}}[\mathrm{C2}][\mathrm{L}] + k_{\mathrm{d3}}[\mathrm{C3}]$$

$$\frac{\mathrm{d}[\mathrm{C3}]}{\mathrm{d}t} = k_{\mathrm{a1}}[\mathrm{C2}][\mathrm{L}] - k_{\mathrm{d3}}[\mathrm{C3}]$$

For the more complicated reactions set expressed by Eq. (3) these differential equations read:

$$\frac{\mathrm{d}[\mathrm{P}]}{\mathrm{d}t} = -k_{\mathrm{a3}}[\mathrm{P}][\mathrm{L}] + k_{\mathrm{d1}}[\mathrm{C1}]$$

$$\begin{aligned} \frac{\mathrm{d}[\mathrm{L}]}{\mathrm{d}t} = &-k_{\mathrm{a3}}[\mathrm{P}][\mathrm{L}] + k_{\mathrm{d1}}[\mathrm{C1}] - k_{\mathrm{a2}}[\mathrm{C1}][\mathrm{L}] + k_{\mathrm{d2}}[\mathrm{C2}] \\ &- k_{\mathrm{a2}}[\mathrm{K1}][\mathrm{L}] + k_{\mathrm{d1}}[\mathrm{C1K1}] - k_{\mathrm{a1}}[\mathrm{C2}][\mathrm{L}] + k_{\mathrm{d3}}[\mathrm{C3}] \\ &- k_{\mathrm{a1}}[\mathrm{C1K1}][\mathrm{L}] + k_{\mathrm{d2}}[\mathrm{C2K1}] - k_{\mathrm{a1}}[\mathrm{K2}][\mathrm{L}] \\ &+ k_{\mathrm{d1}}[\mathrm{C1K2}] \end{aligned}$$

$$\frac{d[C1]}{dt} = k_{a3}[P][L] - k_{d1}[C1] - k_{f1}[C1] + k_{b1}[K1] - k_{a2}[C1][L] + k_{d2}[C2]$$

$$\frac{d[K1]}{dt} = k_{f1}[C1] - k_{b1}[K1] - k_{a2}[K1][L] + k_{d1}[C1K1]$$

$$\frac{d[C2]}{dt} = k_{a2}[C1][L] - k_{d2}[C2] - k_{f2}[C2] + k_{b1}[C1K1] - k_{a1}[C2][L] + k_{d3}[C3]$$

$$\frac{d[C1K1]}{dt} = k_{a2}[K1][L] - k_{d1}[C1K1] + k_{f2}[C2] - k_{b1}[C1K1] - k_{f1}[C1K1] + k_{b2}[K2] - k_{a1}[C1K1][L] + k_{d2}[C2K1]$$

$$\frac{d[K2]}{dt} = k_{f1}[C1K1] - k_{b2}[K2] - k_{a1}[K2][L] + k_{d1}[C1K2]$$

$$\frac{d[C3]}{dt} = k_{a1}[C2][L] - k_{d3}[C3] - k_{f3}[C3] + k_{b1}[C2K1]$$

$$\frac{d[C2K1]}{dt} = k_{a1}[C2K1][L] - k_{d2}[C2K1] + k_{f3}[C3] - k_{b1}[C2K1] - k_{f2}[C2K1] + k_{b2}[C1K2]$$

$$\frac{d[C1K2]}{dt} = k_{a1}[K2][L] - k_{d1}[C1K2] + k_{f2}[C2K1] - k_{b2}[C1K2] - k_{f1}[C1K2] + k_{b3}[K3]$$

$$\frac{d[K3]}{dt} = k_{f1}[C1K2] - k_{b3}[K3]$$

The basic adjustable parameters of both models are the rate constants (12 parameters at the most), and the "molar" fluorescence of different forms of the PNP–guanine complex (9 parameters at the most). The "molar" fluorescence of free protein and free ligand were measured in independent experiments and their values were taken as constants of the model. For the protein, as there is some possibility for damage during preparation, the F_P value was taken as that estimated at the day of measurements. In the case of guanine ligand the assumed value of F_L is average over all experiments—it is about 3000 smaller than the estimated values of the F_P. Besides the rate constants and "molar" fluorescence, there are several other adjustable parameters in our programs. These are offset level for each individual transient, correction factor for the protein concentration, common for all kinetic transients registered with the same protein solution, and correction factors for concentration of the ligand, separate for each kinetic transient, as the solutions of the ligand are subjects of possible errors, a priori different in each individual case. These additional adjustable parameters allow us improve quality of the fits and also when values of these correction factors resulting from the fits are not reasonable, this might indicate some significant problems with our experimental data.

Kinetic traces registered with the stopped-flow apparatus were fitted using a nonlinear numerical integration method based on the least-square deviations criterion. The above models were fitted to the experimental data assuming several possibilities regarding treatment of the rate constants and the optical parameters. For the simpler reaction scheme described by Eq. (2) two possibilities were considered:

(A) The rate constants were fitted with the requirement that they are restricted by the relations: k_{a3}:k_{a2}:k_{a1}=k_{d3}:k_{d2}:k_{d1}=3:2:1. Therefore practically there are only 2 rate constants free to adjust to the model. The "molar" fluorescence of the three possible forms of the complex were freely adjusted.
(B) All the rate constants and all the molar fluorescence of the different forms of the PNP–guanine complex are treated as independent adjustable parameters.

For the more complex reaction scheme described by Eq. (3) four possibilities were considered.

(C) The rate constants were fitted with the requirement that they are restricted by the relations: k_{a3}:k_{a2}:k_{a1}=k_{d3}:k_{d2}:k_{d1}=k_{f3}:k_{f2}:k_{f1}=k_{b3}:k_{b2}:k_{b1}=3:2:1. Therefore practically there are only 4 rate constants free to adjust to the model. The "molar" optical signals of the complexes were assumed to be equal to a sum of "molar fluorescence of the free protein and the appropriate multiplications of two increments, ΔF_b for binding by one site and ΔF_t for conformational transition of the occupied site, with multiplication factors I and J, which are the number of bound guanine molecules, and the number of occupied binding sites which underwent conformational transition, respectively. Therefore practically there are only 2 optical adjustable parameters.
(D) As variant C of the fitting but with all 9 molar fluorescence of the complexes treated as independent adjustable parameters.
(E) As variant C of the fitting but with all 12 rate constants treated as independent adjustable parameters.
(F) All the rate constants and all the molar fluorescence of the different forms of the PNP–guanine complex are treated as independent adjustable parameters.

3. Results and discussion

Table 1 and Fig. 2 present an example of fitting models A–F to a set of kinetic traces registered for mixing 0.77

Table 1
Results of fitting models A–F of PNP–guanine association to the kinetic traces registered for ionic strength of 100 mM

Model parameter	Model of association (see text)					
	A	B	C	D	E	F
k_{a1}	3.07	1.33	7.64	5.13	5.40	5.02
k_{a2}	6.14	14.8	15.3	10.3	25.9	9.17
k_{a3}	9.21	6.09	22.9	15.4	17.4	15.1
k_{d1}	0.09	0.47	0.36	1.31	0.12	2.54
k_{d2}	0.18	0.88	0.72	2.61	2.34	0.95
k_{d3}	0.26	0.35	1.08	3.92	1.70	10.5
k_{f1}	–	–	0.63	1.22	3.37	1.17
k_{f2}	–	–	1.26	2.43	0.97	2.84
k_{f3}	–	–	1.89	3.65	1.44	4.24
k_{b1}	–	–	1.56	0.97	1.22	0.78
k_{b2}	–	–	3.11	1.94	3.93	2.10
k_{b3}	–	–	4.67	2.92	2020.	2.07
F_{C1}	1.32	1.41	1.15	1.19	1.15	1.22
F_{K1}	–	–	1.26	1.43	1.27	1.43
F_{C2}	1.39	1.43	1.30	1.42	1.30	1.41
F_{C1K1}	–	–	1.40	1.48	1.42	1.48
F_{K2}	–	–	1.51	1.48	1.55	1.45
F_{C3}	1.52	1.53	1.45	1.43	1.45	1.43
F_{C2K1}	–	–	1.55	1.50	1.57	1.51
F_{C1K2}	–	–	1.66	1.57	1.70	1.53
F_{K3}	–	–	1.76	1.55	1.83	1.60
rmsd	0.030	0.026	0.029	0.0063	0.0063	0.0057

The association rate constants are given in [μM^{-1} s^{-1}], the remaining rate constants are given in [s^{-1}], and the fluorescence parameters are relative quantities assuming fluorescence of 1 μM protein solution as the unit (F_L=0.00035); rmsd values are also given as relative to the signal of the pure protein solution.

μM (as a trimer) solution of PNP with guanine solutions of concentrations of 1.25, 2.5, 5.0, 10.0 20.0 and 30.0 μM, for ionic strength of 100 mM. Molar fluorescence of free PNP and free guanine at given solution conditions and stopped-flow spectrofluorimeter setup were determined in independent measurements and were kept constant during fitting (for the case of experiment presented in Table 1 and Fig. 2, F_P=2.262 [V μM^{-1}] and F_L=0.0008 [V μM^{-1}]). For clarity of the figure only transients registered for ligand concentrations of 1.25, 2.5, and 30.0 μM are shown, because the transients for the concentration of 5 μM and higher start to overlap with each other at the plateau region. Similar results regarding quality of the fits were obtained for the remaining ionic strength of solutions considered in this work.

Fig. 2 illustrates certain general feature of the experimental data, that it is not possible using models A, B and C to obtain satisfactory simultaneous fits to the transients registered for several ligand concentrations. For models A and B, the fits are acceptable for low ligand concentrations but they are bad for the higher concentrations. On the other hand, for model C it is opposite, the fits for higher concentrations of ligand are satisfactory but for the lower concentrations there are substantial deviations visible. Starting from different initial values of the parameters results in similar behavior. It can be concluded that assumption of one-step association reaction for each binding site is not justifiable and one needs a two-step association model. Model C is of such a type but the fit is also not satisfactory. The fact that it is not possible to obtain satisfactory simultaneous fit to all six transients with model C, which is a two step-binding model for each site, suggests that either requirement of the relation 3:2:1=$k_{\alpha3}$:$k_{\alpha2}$:$k_{\alpha1}$ (α=a, d, f or b) or additivity of optical responses for subsequent binding and conformational transitions are not appropriate for PNP–guanine system. Subsequently one can notice that for models D, E and F, the fits, regarding average overall root-mean-square-deviation (rmsd) and comparability of the fits for all individual transients, are satisfactory. The best fits obtained with models D–F have rmsd values approximately 5 times smaller than the best fits obtained with models A–C. However, because of the relatively large number of adjustable parameters and possibly because the division of guanine binding by each site in a two-step process is not sufficiently well defined, it is not easy to obtain such values of the parameters which give a clear picture of the PNP–guanine binding. Out of the three models D, E and F, only D and F will be discussed further, as for model E, the restrictions imposed on the "molar" fluorescence of different forms of the complexes results in large shifts of apparently accidental "selected" rates towards extremely large or extremely low values. Example of this behavior is given in column "E" of Table 1.

Fitting models D and F to the experimental data was done using the following procedure. First, a number of fits of model C was done and the runs resulting with smallest possible rmsd were selected. Parameters values resulting from these fits were averaged and their standard deviations were estimated. From the ranges of parameters values determined by these mean values and their standard deviations, six sets of initial parameters values were selected for fitting model D to the experimental data. The results of these six fits were used to determine average values of the parameters and their standard deviations. And again they formed the ranges of values from which six sets of starting values of parameters for fitting model F were selected.

Fig. 3 shows an example of fitting model D to the experimental data registered at ionic strength of 50 mM. It can be seen that in principle the fits reflect transition in the character of the transients on going from low to high ligand concentration. Subsequently, Fig. 4 and Table 2 present average results of the above procedure with respect to model D. Fig. 4 presents average values and standard deviations of the four different kinds of the rate constants, $k_{\alpha1}$ with α=a, d, f and b, obtained from fitting model D to the kinetic traces registered at different ionic strength of the solutions. It can be noticed that variation of the values is quite significant, what reflects well known problems with nonlinear fitting, nevertheless one can put a hypothesis that no dependence on the ionic strength is visible. This, if true, would mean that electrostatic interactions play no significant role in the association and dissociation processes. Therefore one can

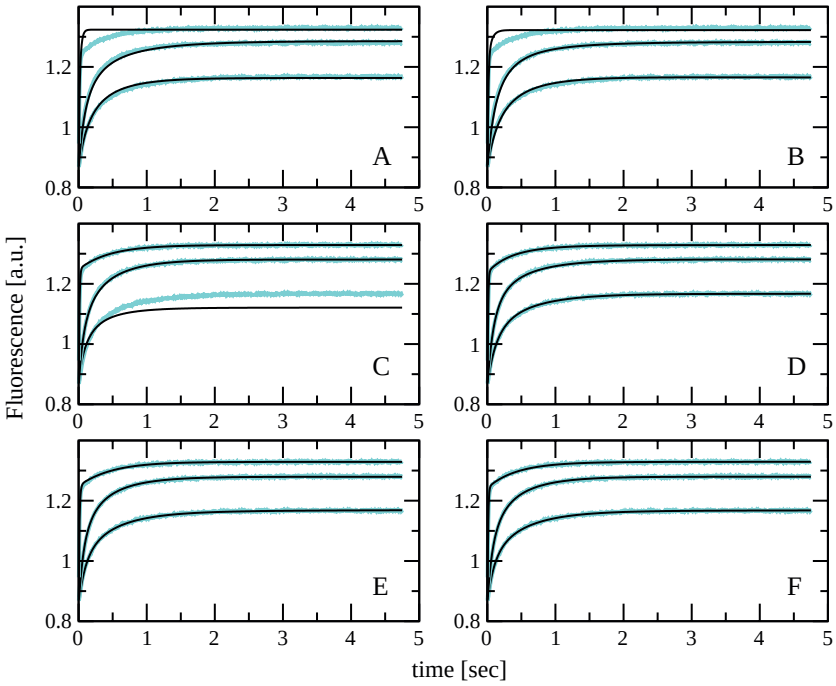

Fig. 2. Example of simultaneous fits, represented by black continuous lines, of models A–F to the set of kinetic traces, represented by noisy lines, registered in the stopped-flow spectrofluorimeter, after mixing of PNP solution with concentration of 0.77 μM (per trimer) with solutions of guanine, with the concentrations of the ligand 1.25, 2.5, 5, 10, 20 and 30 μM, at ionic strength of 100 mM. Only transients for guanine concentrations of 1.25, 2.5 and 30 μM are shown for clarity of the picture, as the transients for 5, 10, 20 and 30 μM overlap with each other in the most parts.

conclude that a neutral form of guanine is bound and dissociated by PNP.

Table 2 shows average increments in molar fluorescence accompanying different binding and transformation processes obtained from model D. These quantities can be used in discussing interactions between the sites as reflected in the optical properties of the complexes. For model C it is assumed that there are two increments describing fluorescence of PNP–guanine complexes, one for binding by a given site and the other for a conformational transformation following the binding. Although the fits are not satisfactory, the values of the increments obtained from different simulations are quite the same for the binding step and for the transformation step, respectively, namely the average values are ΔF_{bind}=0.367±0.027 and ΔF_{tran}=0.144±0.013, at the confidence 95%. When the molar fluorescence of all the complexes can be adjusted independently as in model D, the quality of the fits increases significantly, and the linear dependence imposed by model C disappears. This indicates that each binding site "feels" the state of the two remaining sites. However, the results are somewhat scattered. Table 2 shows that only three fluorescence increments have the values established pretty well by fitting experimental data with model D. These are the fluorescence increments on going from P to C1, from C1 to K1 and from C1 to C2. The remaining values are smaller and with larger standard deviations. However, it can be concluded that changes in fluorescence of complexes after the second ligand is bound are small, i.e. all forms beginning from C2 and C1K1 change their fluorescence not significantly upon next binding and/or conformational transition. This result is surprising and might indicate that either imposed restriction for relation between the rate constants in model D or that the

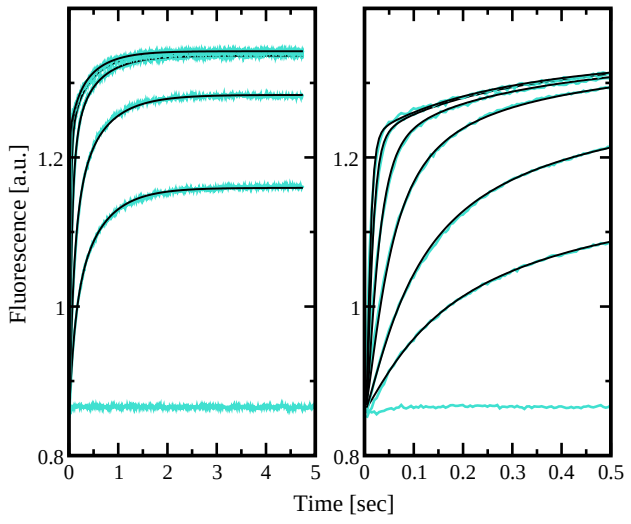

Fig. 3. Example of fitting model D (smooth thin lines) to kinetic traces (curved noisy lines) obtained in the stopped-flow spectrofluorimeter, after mixing of PNP solution with concentration of 0.77 μM (per trimer) with solutions of guanine, for the concentrations of the ligand: (from bottom to top) 1.25, 2.5, 5.0, 10.0, 20.0 and 30.0 μM, at ionic strength of 50 mM. The flat noisy line was registered for mixing PNP solution with equal volume of the buffer. The left side shows the whole registered transients, the right part shows the first 0.5 s of the transients.

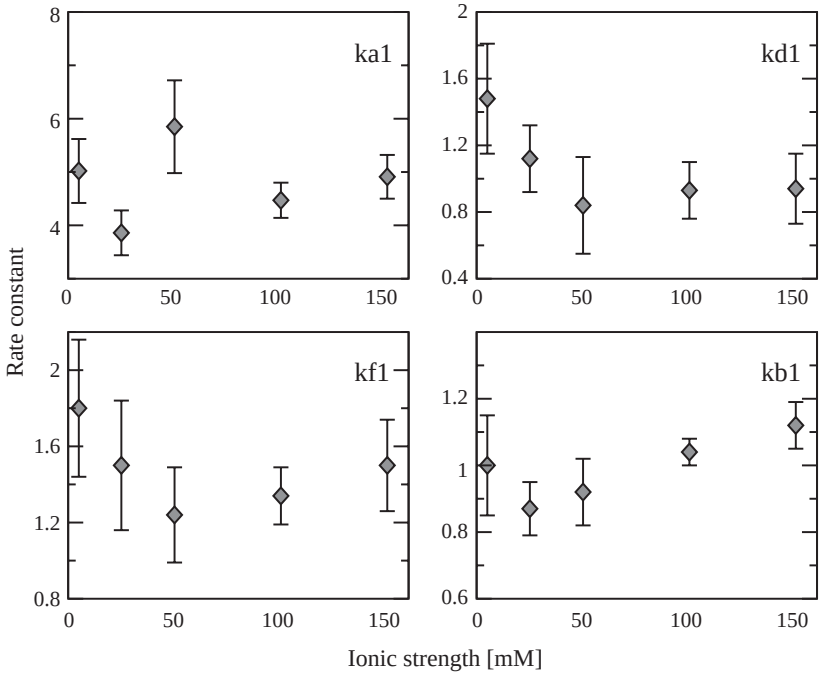

Fig. 4. Average rate constants $\boldsymbol{k}_{\alpha,i}$ obtained from model D for different ionic strength. The $\boldsymbol{k}_{a1}$ are given in [μM^{-1} s^{-1}], and the remaining rate constants are given in [s^{-1}].

division of the binding into two steps is not well defined, the different forms are not separated by significant energy barriers. The first possibility was tested by application of model F.

Fig. 5 shows an example of fitting our experimental data with model F. Again it can be noted that transition from monophasic, for low ligand concentrations, to biphasic, for high concentrations, character of the transients is well reproduced by the fits, although the improvement of the fits in comparison to results obtained with model D is rather small. The average results obtained from six initial sets of parameters, as described above, are summarized in Tables 3 and 4. It can be noted from Table 3, that there are some regularities. The first is that k_{d2} is smaller than both k_{d1} and k_{d3} indicating that dissociation of the ligand when two sites are occupied is less probable. The next observations is that k_{a2}, k_{b1} are ionic strength independent. From Table 4 it can be seen the values of fluorescence change upon different step in the reaction scheme represented by Eq. (3) are rather not more regular than in from Table 2. Obviously the increased number of adjustable parameters in model F in comparison to model D makes the problem of obtaining reliable values of these parameters from fits to the experimental data more difficult. On the other hand, there are some correlations between the parameters and in order to minimize effects of these correlations one needs some additional data which allow imposing of restriction on some parameters. One such possibility is in determination of the association rate constants k_{ai} by methods of Brownian dynamics [13,14]. Another possibility is to perform other

Table 2
Relative changes in fluorescence as predicted by results of fitting model D of PNP–guanine association to the kinetic traces for different ionic strength of solution

Molecular process	Ionic strength [mM]				
	5	25	50	100	150
P→C1	0.22±0.03	0.28±0.03	0.13±0.05	0.21±0.02	0.21±0.02
C1→K1	0.17±0.07	0.15±0.07	0.39±0.13	0.19±0.04	0.19±0.06
C2→C1K1	0.04±0.08	0.05±0.03	−0.05±0.04	0.00±0.03	−0.04±0.03
C1K1→K2	0.07±0.15	−0.03±0.06	0.13±0.05	0.04±0.03	0.04±0.02
C3→C2K1	0.19±0.03	0.12±0.03	0.11±0.03	0.08±0.01	0.09±0.02
C2K1→C1K2	−0.02±0.05	0.01±0.03	0.02±0.05	0.04±0.01	0.01±0.04
C1K2→K3	0.06±0.08	0.05±0.02	0.06±0.09	0.06±0.04	0.08±0.10
C1→C2	0.28±0.02	0.23±0.02	0.30±0.01	0.23±0.01	0.24±0.02
K1→C1K1	0.14±0.10	0.12±0.06	−0.14±0.15	0.04±0.03	0.00±0.06
C2→C3	−0.04±0.04	−0.05±0.02	0.00±0.05	−0.02±0.01	−0.05±0.02
C1K1→C2K1	0.11±0.10	0.03±0.06	0.17±0.06	0.06±0.02	0.08±0.04
K2→C1K2	0.02±0.11	0.08±0.03	0.05±0.06	0.07±0.02	0.05±0.03

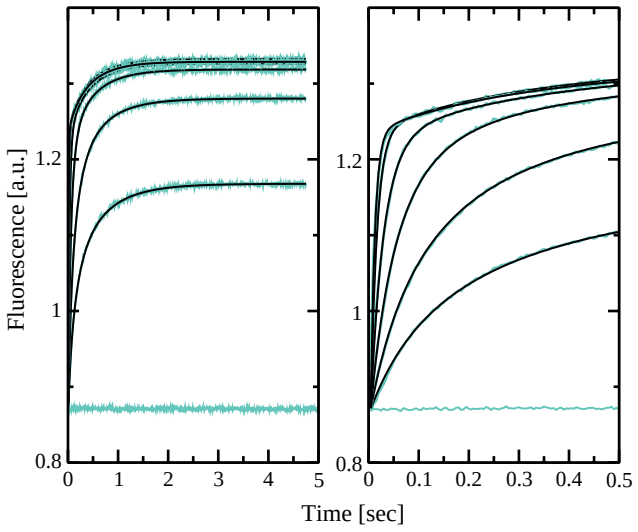

Fig. 5. Example of fitting model F (smooth thin lines) to kinetic traces (curved noisy lines) obtained in the stopped-flow spectrofluorimeter, after mixing of PNP solution with concentration of 0.77 μM (per trimer) with solutions of guanine, for the concentrations of the ligand: (from bottom to top) 1.25, 2.5, 5.0, 10.0, 20.0 and 30.0 μM, at ionic strength of 100 mM. The flat noisy line was registered for mixing PNP solution with equal volume of the buffer. The left side shows the whole registered transients, the right part shows the first 0.5 s of the transients.

kinds of experiments which can be explained by models like the one represented by Eq. (3), for example dissociation kinetic experiments. Simultaneous fitting of kinetics transients obtained in both association and dissociation experiments may help to establish less scattered values of parameters of the reaction models. These possibilities will be explored in a further study. We will end this discussion with an analysis of microscopic dissociation constants, which allow us to make a comparison with some previous studies of PNP.

As described in Materials and methods, protein concentration was calculated from UV absorption measurements. Concentration of the active enzyme form was also determined in the independent experiments. It was done by comparing, for each sample prepared for the stopped-flow experiments, PNP enzymatic activity vs. inosine (see Materials and methods) with the specific activity of the fully active enzyme (34 U/mg [3]). Such a value was usually 10–20% lower than that from UV measurements. However, it is not clear if activity vs. inosine is fully correlated with binding of guanine. Therefore in fitting models to experimental data both hypothesis were tested: protein concentration from UV absorption or from activity measurements were used. In the later case 2–3 fold higher rmsd were typically obtained. Moreover in this case the program tends to increase the value of protein concentration from that assumed to be in the range 80–90%, although the final fitted values are below 100%. This probably results from well known problems with nonlinear least squares fittings. Taking all this into account we conclude that there is no enough experimental data to judge which method of protein concentration calculation is more correct for analyzing stopped-flow kinetic experiments. However, fortunately this only affects the fitted values of kinetic and optical parameters but has no influence on the final conclusion which binding model (A–F) is appropriate for describing PNP–guanine complex formation.

As the last point of this section the problem of equilibrium dissociation constants will be discussed. The reaction scheme presented in Eq. (3) allows one to define six microscopic dissociation constants characterizing a dissociation process of ligand molecule from given particular binding site with fixed forms of the two remaining binding sites. These dissociation constants are presented in Table 5. The upper part of this table shows overall dissociation constants characterizing two-step dissociation reaction, and the lower part of the table shows, in the corresponding sequence, the one-step components of these full reactions, which correspond to dissociation of a ligand from binding

Table 3
Example of results of fitting model F of PNP–guanine association to the kinetic traces registered at different ionic strength of solution

Model parameter	Ionic strength [mM]				
	5	25	50	100	150
k_{a1}	2.20±1.22	4.16±0.68	8.76±1.78	4.73±1.05	7.18±1.22
k_{a2}	10.3±0.95	10.7±0.90	12.0±1.40	9.23±0.48	10.4±1.40
k_{a3}	24.2±1.40	12.8±0.70	15.0±0.40	15.4±0.30	13.1±0.90
k_{d1}	3.27±0.63	2.96±0.25	3.18±0.48	2.71±0.41	2.51±0.31
k_{d2}	1.66±1.56	0.79±0.50	0.55±0.33	0.96±0.39	1.04±0.84
k_{d3}	3.13±2.74	7.73±2.09	12.2±3.00	8.09±2.47	4.25±1.31
k_{f1}	1.68±0.49	1.84±0.14	1.87±0.17	1.28±0.08	2.43±0.51
k_{f2}	4.24±1.14	2.44±0.52	2.69±0.44	2.76±0.48	5.18±1.76
k_{f3}	5.87±0.93	4.77±1.99	3.85±0.23	5.27±1.92	4.36±0.49
k_{b1}	0.53±0.12	0.57±0.03	0.50±0.07	0.79±0.15	0.64±0.08
k_{b2}	1.21±0.44	2.79±0.52	5.43±0.66	1.92±0.10	6.81±0.99
k_{b3}	3.09±0.44	2.71±0.79	1.55±0.04	2.25±0.29	2.04±0.21
⟨rmsd⟩	0.01335	0.01229	0.01397	0.01113	0.01228

The association rate constants are given in [$\mu M^{-1}\ s^{-1}$], the remaining rate constants are given in [s^{-1}]; rmsd values are given as relative to the signal of the pure protein solution.

Table 4
Relative changes in fluorescence as predicted by results of fitting model F of PNP–guanine association to the kinetic traces for different ionic strength of solution

Molecular process	Ionic strength [mM]				
	5	25	50	100	150
P→C1	0.16±0.01	0.28±0.02	0.17±0.01	0.21±0.01	0.25±0.03
C1→K1	0.17±0.05	0.15±0.02	0.27±0.04	0.22±0.03	0.12±0.05
C2→C1K1	0.15±0.04	0.15±0.04	−0.14±0.02	0.08±0.02	−0.03±0.04
C1K1→K2	−0.01±0.05	−0.09±0.04	0.32±0.04	−0.04±0.02	0.00±0.05
C3→C2K1	0.11±0.02	0.10±0.02	0.14±0.01	0.08±0.02	0.11±0.01
C2K1→C1K2	0.03±0.02	0.03±0.02	−0.08±0.01	0.03±0.01	−0.07±0.01
C1K2→K3	0.05±0.02	0.06±0.03	0.17±0.01	0.08±0.01	0.14±0.01
C1→C2	0.29±0.02	0.16±0.01	0.28±0.01	0.20±0.01	0.19±0.02
K1→C1K1	0.26±0.10	0.16±0.04	−0.13±0.05	0.06±0.01	0.04±0.08
C2→C3	0.05±0.02	0.03±0.02	−0.03±0.02	0.01±0.01	−0.05±0.01
C1K1→C2K1	0.02±0.06	−0.01±0.02	0.25±0.04	0.01±0.02	0.08±0.06
K2→C1K2	0.06±0.04	0.11±0.02	−0.14±0.04	0.08±0.03	0.02±0.04

site which did not undergo conformational transformation. In the case of model D, because of the assumed relations between the microscopic rate constants, all these six dissociation constants, either two-step or one-step, reduce to just one value. For model F in principle all six microscopic dissociation constants may have different values. These dissociation constants are presented in Table 5. It can be seen that all dissociation equilibrium constants are in the range between a hundredth part and one μM. The other thing which can be noted that, with only 3 exceptions, the overall dissociation constants are smaller than their one-step counterparts, what indicates anticipated stabilizing role of the conformational transition following initial binding of ligand.

Results presented in this work can be compared with those obtained by Porter [2] for PNP–guanine association based on titration of enzyme fluorescence with the ligand and on the stopped-flow experiments. Results reported by Porter were obtained on the basis of a model considering only total active site concentration of PNP i.e. neglecting the fact that these active sites are organized into trimers. The author determined observed rate constants, k_{obs} from kinetic transients registered in the stopped-flow experiments, and based on the dependence of k_{obs} on guanine concentration he obtained bimolecular association constant of 7.8±0.2 μM^{-1} s^{-1}. The dissociation rate constant was estimated as 1.1±0.1 s^{-1}. Both these results gave dissociation equilibrium constant K_d=0.14 μM. On the other hand K_d=0.08±0.02 μM was obtained in the same work based on titration of enzyme fluorescence with the ligand. All these values are close to the values obtained by the present authors.

Acknowledgements

We thank Lucyna Magnowska for excellent technical assistance. This work was supported by the State

Table 5
Microscopic dissociation constants in [μM] obtained from models D and F

Dissociation process	Formula for dissociation constant	Ionic strength in [mM]					Model of reaction
		5	25	50	100	150	
Two-step process							
All	$k_{b1}k_{d1}/k_{a1}k_{f1}$	0.16	0.17	0.11	0.16	0.14	D
K3→K2	$k_{b3}k_{d1}/3k_{a1}k_{f1}$	0.91	0.35	0.10	0.34	0.10	F
K2→K1	$k_{b2}k_{d1}/k_{a2}k_{f1}$	0.23	0.42	0.77	0.44	0.68	F
K1→P	$3k_{b1}k_{d1}/k_{a3}k_{f1}$	0.13	0.21	0.17	0.33	0.15	F
C1K2→C1K1	$k_{b2}k_{d2}/2k_{a1}k_{f2}$	0.11	0.11	0.06	0.07	0.10	F
C1K1→C1	$2k_{b1}k_{d2}/k_{a2}k_{f2}$	0.04	0.03	0.02	0.06	0.02	F
C2K1→C2	$k_{b1}k_{d3}/k_{a1}k_{f3}$	0.13	0.22	0.18	0.26	0.09	F
One-step process							
All	k_{d1}/k_{a1}	0.29	0.29	0.14	0.21	0.19	D
C1K2→K2	k_{d1}/k_{a1}	1.49	0.71	0.36	0.57	0.35	F
C1K1→K1	$2k_{d1}/k_{a2}$	0.64	0.55	0.53	0.59	0.48	F
C1→P	$3k_{d1}/k_{a3}$	0.41	0.69	0.64	0.53	0.57	F
C2K1→C1K1	$k_{d2}/2k_{a1}$	0.38	0.10	0.03	0.10	0.07	F
C2→C1	k_{d2}/k_{a2}	0.16	0.07	0.05	0.10	0.10	F
C3→C2	$k_{d3}/3k_{a1}$	0.47	0.62	0.46	0.57	0.29	F

Committee for Scientific Research, Poland (KBN, Grant No. 6P04A00121).

References

[1] A. Bzowska, E. Kulikowska, D. Shugar, Purine nucleoside phosphorylase: properties, functions and clinical aspects, Pharmacol. Ther. 88 (2000) 349–425.
[2] D.J.T. Porter, Purine nucleoside phosphorylase. Kinetic mechanism of the enzyme from calf spleen, J. Biol. Chem. 267 (1992) 7342–7351.
[3] A. Bzowska, Calf spleen purine nucleoside phosphorylase: complex kinetic mechanism, hydrolysis of 7-methylguanosine and oligomeric state in solution, Biochim. Biophys. Acta 1596 (2002) 293–317.
[4] G. Koellner, M. Luić, D. Shugar, W. Saenger, A. Bzowska, Crystal structure of calf spleen purine nucleoside phosphorylase in a complex with hypoxanthine at 2.15 Å resolution, J. Mol. Biol. 265 (1997) 202–216.
[5] B. Wielgus-Kutrowska, A. Bzowska, J. Tebbe, G. Koellner, D. Shugar, Purine nucleoside phosphorylase (PNP) from Cellulomonas sp.: physico-chemical properties, and binding of substrates determined by ligand-dependent enhancement of enzyme intrinsic fluorescence, and by protective effects of ligands on thermal inactivation of the enzyme, Biochim. Biophys. Acta 1597 (2002) 320–334.
[6] K. Hemminki, Fluorescence properties of alkylated guanine derivatives, Acta Chem. Scand., B 34 (1984) 603–605.
[7] S.P. Assenza, P.R. Brown, Ultraviolet and fluorescence characterization of purines and pyrimidines by post-column pH manipulation, J. Chromatogr. 289 (1984) 355–365.
[8] J. Tebbe, A. Bzowska, B. Wielgus-Kutrowska, Z. Kazimierczuk, W. Schröder, D. Shugar, W. Saenger, G. Koellner, Crystal structure of the purine nucleoside phosphorylase (PNP) from Cellulomonas sp. and its implication for the mechanism of trimeric PNPs, J. Mol. Biol. 294 (1999) 1239–1255.
[9] A. Bzowska, G. Koellner, B. Wielgus-Kutrowska, A. Stroh, G. Raszewski, A. Holý, T. Steiner, J. Frank, Crystal structure of calf spleen purine nucleoside phosphorylase with two full trimers in the asymmetric unit: important implications for the mechanism of catalysis, J. Mol. Biol. 342 (2004) 1015–1032.
[10] J.D. Stoeckler, R.P. Agarwal, K.C. Agarwal, R.E. Parks Jr., Purine nucleoside phosphorylase from human erythrocytes, Methods Enzymol. 51 (1978) 530–538.
[11] M. Długosz, E. Bojarska, J.M. Antosiewicz, A procedure for analysis of stopped-flow transients for protein-ligand association, J. Biochem. Biophys. Methods 51 (2002) 179–193.
[12] W. Humphrey, A. Dalke, K. Schulten, VMD-visual molecular dynamics, J. Mol. Graph. 44 (1996) 33–38.
[13] M.E. Davis, J.D. Madura, B.A. Luty, J.A. McCammon, Electrostatics and diffusion of molecules in solution: simulations with the University of Houston Brownian Dynamics program, Comput. Phys. Commun. 62 (1991) 187–197.
[14] J. Antosiewicz, M.K. Gilson, I.H. Lee, J.A. McCammon, Acetylcholinesterase: diffusional encounter rate constants for dumbbell models of ligand, Biophys. J. 68 (1995) 62–68.